International Journal of Fracture **100:** 207–225, 1999.

Variation of mixed modes stress intensity factors of an inclined semi-elliptical surface crack

NAO-AKI NODA, KIMIHIRO KOBAYASHI and MAKOTO YAGISHITA
Mechanical Engineering Department, Kyushu Institute of Technology, 1-1 Sensui-cho, Tobataku, Kitakyushu 804-8550, Japan. e-mail: noda@mech.kyutech.ac.jp

Received 5 January 1998; accepted in revised form 20 July 1998

Abstract. In this paper, a singular integral equation method is applied to calculate the stress intensity factor along crack front of a 3D inclined semi-elliptical surface crack in a semi-infinite body under tension. The stress field induced by displacement discontinuities in a semi-infinite body is used as the fundamental solution. Then, the problem is formulated as a system of integral equations with singularities of the form r^{-3}. In the numerical calculation, the unknown body force doublets are approximated by the product of fundamental density functions and polynomials. The results show that the present method yields smooth variations of mixed modes stress intensity factors along the crack front accurately for various geometrical conditions. The effects of inclination angle, elliptical shape, and Poisson's ratio are considered in the analysis. Crack mouth opening displacements are shown in figures to predict the crack depth and inclination angle. When the inclination angle is 60 degree, the mode I stress intensity factor F_{I} has negative value in the limited region near free surface. Therefore, the actual crack surface seems to contact each other near the surface.

Keywords: Semi-elliptical crack, inclined crack, stress intensity factor, crack opening displacement, singular integral equation, body force method.

Notation

a	major radius of a semi-elliptical crack
b	minor radius of a semi-elliptical crack
(x, y', z')	rectangular coordinate in Figure 1
(x, y, z)	rectangular coordinate in Figure 1
(ξ, η, ζ)	(x, y, z) coordinate where body force is applied
(x_a, y_b)	$(x/a, y/b)$
E	Young modulus
G	Shear modulus
ν	Poisson's ratio
H	$(1-2\nu)/4(1-\nu)^2$
$f_{zz}(\xi, \eta)$, $f_{yz}(\xi, \eta)$, $f_{zx}(\xi, \eta)$	unknown density functions of body force doublet
$w_{zz}(\xi_a, \eta_b)$, $w_{yz}(\xi_a, \eta_b)$, $w_{zx}(\xi_a, \eta_b)$	fundamental density function of body force doublet
(u_x, u_y, u_z)	displacement in (x, y, x) direction
$U_z(x_a, y_b)$	crack opening displacement $= u_z(x_a, y_b, +0) - u_z(x_a, y_b, -0)$
$U_x(x_a, y_b)$	crack opening displacement $= u_y(x_a, y_b, +0) - u_y(x_a, y_b, -0)$

$U_x(x_a, y_b)$	crack opening displacement $= u_x(x_a, y_b, +0) - u_x(x_a, y_b, -0)$
$U_{z'E}(x_a, y_b)$	crack opening displacement of an elliptical crack
$U_{y'E}(x_a, y_b)$	crack opening displacement of an elliptical crack
$U_{x'E}(x_a, y_b)$	crack opening displacement of an elliptical crack
$M_{\mathrm{I}}(x', y')$	$U_z(x_a, y_b)/U_{z'E}(x_a, y_b)$
$M_{\mathrm{II}}(x', y')$	$U_y(x_a, y_b)/U_{y'E}(x_a, y_b)$
$M_{\mathrm{III}}(x', y')$	$U_x(x_a, y_b)/U_{x'E}(x_a, y_b)$
β	eccetric angle of ellipse
$K_{\mathrm{I}}(\beta)$, $K_{\mathrm{II}}(\beta)$, $K_{\mathrm{III}}(\beta)$	stress intensity factors along the crack front
$K_{\mathrm{I}E}(\beta)$, $K_{\mathrm{II}E}(\beta)$, $K_{\mathrm{III}E}(\beta)$	stress intensity factors of an elliptical crack
$M_{\mathrm{I}}(\beta)$, $M_{\mathrm{II}}(\beta)$, $M_{\mathrm{III}}(\beta)$	dimensionless stress intensity factors $F_i(\beta) = K_i(\beta)/\sigma_z'^{\infty}\sqrt{\pi h}$ $i = \mathrm{I}, \mathrm{II}, \mathrm{III}$
$F_{\mathrm{I}}(\beta)$, $F_{\mathrm{II}}(\beta)$, $F_{\mathrm{III}}(\beta)$	dimensionless stress intensity factors $M_i(\beta) = K_i(\beta)/K_{iE}(\beta)$ $i = \mathrm{I}, \mathrm{II}, \mathrm{III}$

1. Introduction

In most cases, fatigue crack initiation occurs from or near surfaces. Therefore the analysis of the stress intensity factors of 3D surface cracks has contributed in design and maintenance of various structures. Most previous studies have treated mode I type 3D surface cracks because opening type stress intensity factor is known as the dominant parameter controlling final fractures (Nisitani–Murakami, 1974a,b, Isida–Noguchi, 1985a,b, Isids–Tsuru–Noguchi, 1993a,b). However, several practical problems are closely related to mixed mode stress intensity factors for inclined surface cracks. For example, it is well-known that initial fatigue cracks, which is called stage I cracks, are likely to incline about 45 degrees to the loading axis. In addition, in the surfaces subjected to rolling contact loads initial cracks are likely to incline 15-30 degrees to the surface. Then, the propagation stage cracks will be influenced by mixed mode stress intensity factors of those initial-stage-cracks.

Murakami has investigated mixed mode stress intensity factors for inclined semi-elliptical, rectangular, and triangular shaped cracks using body force method (Nisitani, 1967) with triangular element which takes constant value of unknown body force density (Murakami–Isida, 1984; Murakami, 1985). Isida–Tokumoto–Noguchi (1982, 1990) has shown the variation of stress intensity factors for inclined semi-elliptical cracks using body force method with rectangular elements. Murakami and Sakae (1992) also have analyzed 3D kinked surface cracks. In these analyses, however, the weight unknown function has discontinuity along the boundary of elements; then, final results were obtained using extrapolation method.

In the preceding paper, the numerical solutions of the singular integral equation of the body force method in 3D mode I crack has been discussed (Noda–Miyoshi, 1995). In the numerical solutions unknown body force densities have been approximated by the products of fundamental density functions and polynomials. Then, the results show the analytical method yields smooth variation of stress intensity factor and crack opening displacement with higher accuracy compared with other methods. In this study the method will be applied to inclined semi-elliptical surface cracks.

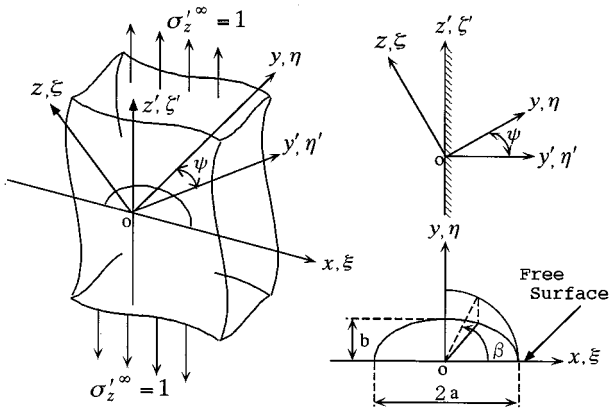

Figure 1. An inclined semi-elliptical surface crack in a semi-infinite body.

2. Singular integral equation of the body force method for a mixed mode surface crack

Consider a semi-infinite body under uniform tension σ'^{∞}_z having an inclined semi-elliptical crack as shown in Figure 1. Here, $z'x$-plane is free from stress, and a semi-elliptical crack with principal diameters 2a and 2b is embedded on the xy plane having an inclination angle ψ to the xy' plane. The body force method is used to formulate the problem as a system of singular integral equations, whose unknowns are densities of body forces $f_{zz}(\xi, \eta)$, $f_{yz}(\xi, \eta)$, $f_{zx}(\xi, \eta)$. Here, (ξ, η, ζ) is a (x, y, z) coordinate where the body force is applied. The body force densities are equivalent to crack opening displacements $U_z(x_a, y_b)$, $(U_x(x_a, y_b), U_x(x_a, y_b)$ as shown in (1e) (Noda–Oda, 1992).

$$\left.\begin{aligned}
&\frac{(1-2\nu)}{8\pi(1-\nu)^2}\left[\iint\!\!\!\!\!\!=_S \frac{f_{zz}(\xi,\eta)}{r_1^3}\,\mathrm{d}\xi\,\mathrm{d}\eta\right.\\
&\qquad\left.+\iint\!\!\!\!\!\!=_S K_{zz}^{f_{zz}}(\xi,\eta,x,y,\psi)\,f_{zz}(\xi,\eta)\,\mathrm{d}\xi\,\mathrm{d}\eta\right]\\
&+\frac{1}{8\pi(1-\nu)}\left[\iint_S K_{zz}^{f_{yz}}(\xi,\eta,x,y,\psi)\,f_{yz}(\xi,\eta)\,\mathrm{d}\xi\,\mathrm{d}\eta\right.\\
&\qquad\left.+\iint_S K_{zz}^{f_{zx}}(\xi,\eta,x,y,\psi)\,f_{zx}(\xi,\eta)\,\mathrm{d}\xi\,\mathrm{d}\eta\right]=-\sigma'^{\infty}_z\cos^2\psi
\end{aligned}\right\} \tag{1a}$$

$$\left.\begin{aligned}
&\frac{1}{8\pi(1-\nu)}\left[\iint\!\!\!\!\!\!=_S \frac{6\nu(x-\xi)(y-\eta)}{r_1^5}\,f_{yz}(\xi,\eta)\,\mathrm{d}\xi\,\mathrm{d}\eta\right.\\
&\qquad+\iint\!\!\!\!\!\!=_S\left\{\frac{2(1-2\nu)}{r_1^3}+\frac{6\nu(y-\eta)^2}{r_1^5}\right\}f_{zx}(\xi,\eta)\,\mathrm{d}\xi\,\mathrm{d}\eta\\
&\qquad+\iint_S K_{yz}^{f_{zz}}(\xi,\eta,x,y,\psi)\,f_{zz}(\xi,\eta)\,\mathrm{d}\xi\,\mathrm{d}\eta\\
&\qquad+\iint_S K_{yz}^{f_{yz}}(\xi,\eta,x,y,\psi)\,f_{yz}(\xi,\eta)\,\mathrm{d}\xi\,\mathrm{d}\eta\\
&\qquad\left.+\iint_S K_{yz}^{f_{zx}}(\xi,\eta,x,y,\psi)\,f_{zx}(\xi,\eta)\,\mathrm{d}\xi\,\mathrm{d}\eta\right]=-\sigma'^{\infty}_z\cos\psi\sin\psi
\end{aligned}\right\} \tag{1b}$$

$$\left.\begin{aligned}
&\frac{1}{8\pi(1-\nu)}\left[\iint\!\!\!\!\!\!=_S\left\{\frac{2(1-2\nu)}{r_1^3}+\frac{6\nu(x-\xi)^2}{r_1^5}\right\}f_{yz}(\xi,\eta)\,\mathrm{d}\xi\,\mathrm{d}\eta\right.\\
&\qquad+\iint\!\!\!\!\!\!=_S\frac{6\nu(x-\xi)(y-\eta)}{r_1^5}f_{zx}(\xi,\eta)\,\mathrm{d}\xi\,\mathrm{d}\eta\\
&\qquad+\iint_S K_{zx}^{f_{zz}}(\xi,\eta,x,y,\psi)\,f_{zz}(\xi,\eta)\,\mathrm{d}\xi\,\mathrm{d}\eta\\
&\qquad+\iint_S K_{zx}^{f_{yz}}(\xi,\eta,x,y,\psi)\,f_{yz}(\xi,\eta)\,\mathrm{d}\xi\,\mathrm{d}\eta\\
&\qquad\left.+\iint_S K_{zx}^{f_{zx}}(\xi,\eta,x,y,\psi)\,f_{zx}(\xi,\eta)\,\mathrm{d}\xi\,\mathrm{d}\eta\right]=0
\end{aligned}\right\} \tag{1c}$$

$$\left.\begin{aligned}
&y=y'/\cos\psi\ \ z=z'/\cos\psi\\
&r_1=\sqrt{(x-\xi)^2+(y'-\eta')^2+(z'-\zeta')^2}\\
&S=\left\{(\xi,\eta)|(\xi/a)^2+(\eta/b)^2\leqslant 1,\eta\geqslant 0\right\}
\end{aligned}\right\} \tag{1d}$$

$$\left.\begin{aligned}
U_z(x_a,y_b) &= u_z(x_a,y_b,+0)-u_z(x_a,y_b,-0)\\
&= \frac{(1-2\nu)(1+\nu)}{E(1-\nu)}f_{zz}(x_a,y_b)\\
U_y(x_a,y_b) &= u_y(x_a,y_b,+0)-u_y(x_a,y_b,-0)\\
&= \frac{2(1+\nu)}{E}f_{yz}(x_a,y_b)\\
U_x(x_a,y_b) &= u_x(x_a,y_b,+0)-u_x(x_a,y_b,-0)\\
&= \frac{2(1+\nu)}{E}f_{zx}(x_a,y_b)
\end{aligned}\right\} \tag{1e}$$

Equations (1a), (1b), (1c) enforce boundary conditions at the prospective boundary S for crack; that is, $\sigma_Z=0, \tau_{yz}=0, \tau_{ZX}=0$. Equation (1) includes singular terms in the form of $1/r_1^3, 1/r_1^5$ corresponding to the ones of an elliptical crack in an infinite body. The notation $\iint\!\!\!\!\!\!=_S$ should be interpreted as a finite part integral (Hadamard, 1923) in the region S. The notation $K_{zz}^{f_{zz}}(\xi,\eta,x,y,\psi)$ means a function that satisfies the boundary condition for free surface.

3. Numerical solution of singular integral equations

In the conventional body force method (Nisitani, 1967), the crack region is divided into several elements and unknown functions of the body force densities have been approximated by using fundamental density functions and step functions. However, the expressions using step functions give rise to singularities along the element boundaries, and they tend to deteriorate the accuracy and validity in sophisticated problems. In the present analysis, the following

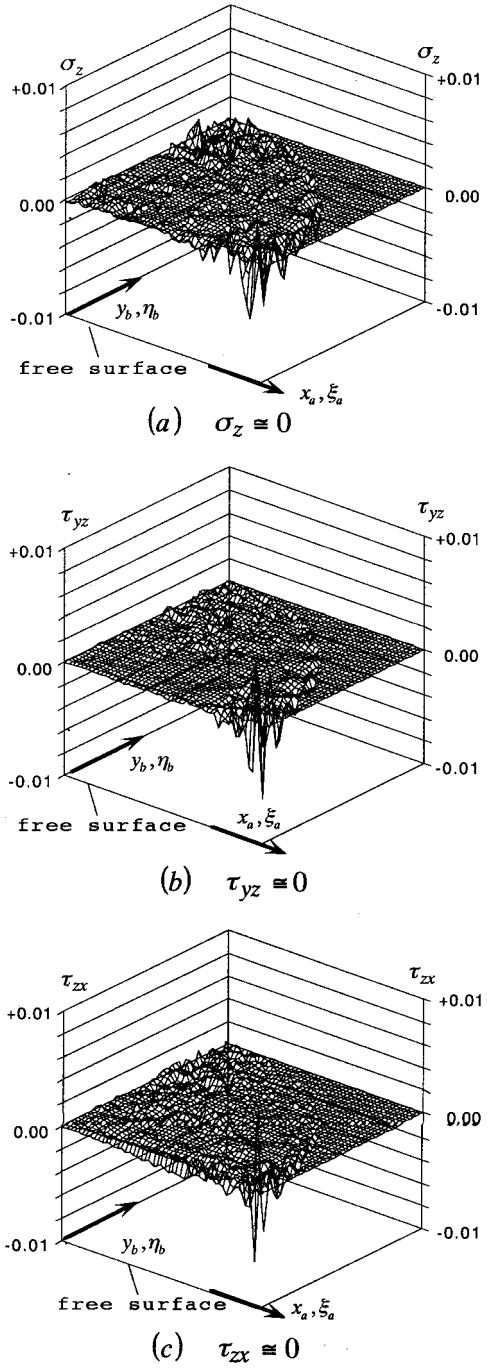

Figure 2. Compliance of boundary condition $\sigma_z = 0$, $\tau_{yz} = 0$, $\tau_{zx} = 0$ in Figure 1 when $n = 20$, $b/a = 1.0$, $\psi = 60°$, $\nu = 0.3$.

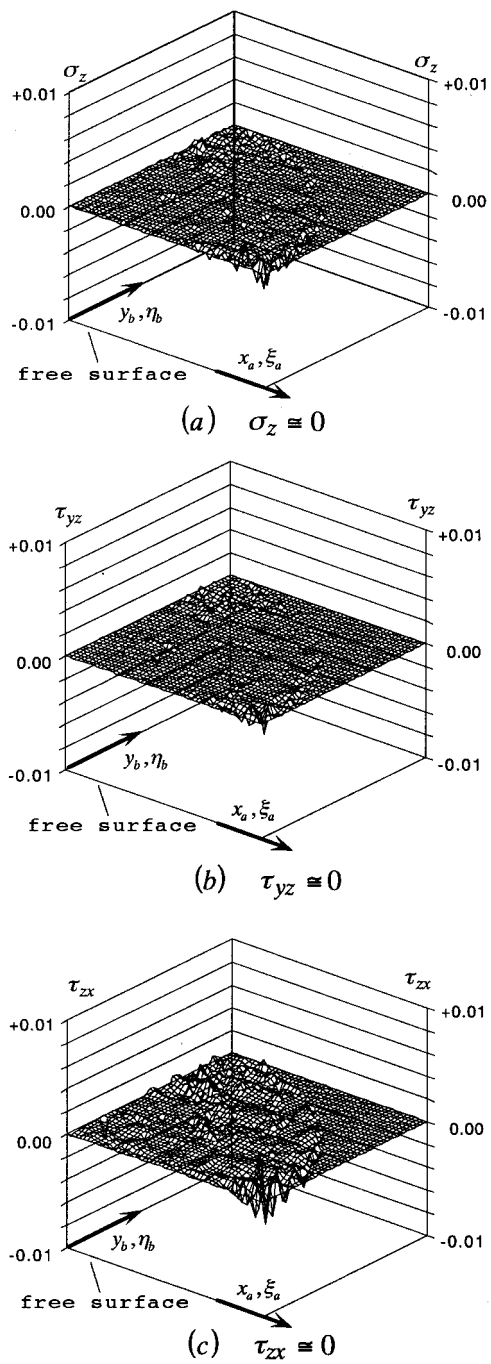

Figure 3. Compliance of boundary condition $\sigma_z = 0$, $\tau_{yz} = 0$, $\tau_{zx} = 0$ in Figure 1 when $n = 20$, $b/a = 1.0$, $\Psi = 60°$, $\nu = 0.0$.

expressions have been used to approximate the unknown functions as continuous functions. First, we put

$$\left.\begin{aligned}
&f_{zz}(\xi,\eta) = F_{zz}(\xi_a,\eta_b)w_{zz}(\xi_a,\eta_b)\\
&f_{yz}(\xi,\eta) = F_{yz}(\xi_a,\eta_b)w_{yz}(\xi_a,\eta_b)\\
&f_{zx}(\xi,\eta) = F_{zx}(\xi_a,\eta_b)w_{zx}(\xi_a,\eta_b)\\
&w_{zz}(\xi_a,\eta_b) = \frac{4(1-\nu)^2 b\sigma_z^{\infty}}{(1-2\nu)E(k)}\sqrt{1-\xi_a^2-\eta_b^2}\\
&w_{yz}(\xi_a,\eta_b) = \frac{2b(1-\nu)k^2\tau_{yz}^{\infty}}{C(k)}\sqrt{1-\xi_a^2-\eta_b^2}\\
&w_{zx}(\xi_a,\eta_b) = \frac{2b(1-\nu)k^2\tau_{zx}^{\infty}}{B(k)}\sqrt{1-\xi_a^2-\eta_b^2}\\
&B(k) = (k^2-\nu)E(k) + \nu k'^2 K(k)\\
&C(k) = (k^2+\nu k'^2)E(k) - \nu k'^2 K(k)\\
&k' = b/a \leqslant 1 \quad k = \sqrt{1-(b/a)^2} \quad \xi_a = \xi/a \quad \eta_b = \eta/b\\
&K(k) = \int_0^{\pi/2} \frac{\mathrm{d}\lambda}{\sqrt{1-k^2\sin^2\lambda}}, \qquad E(k) = \int_0^{\pi/2} \sqrt{1-k^2\sin^2\lambda}\,\mathrm{d}\lambda
\end{aligned}\right\} \tag{2}$$

Here, $w_{zz}(\xi_a,\eta_b)$, $w_{yz}(\xi_a,\eta_b)$, $w_{zx}(\xi_a,\eta_b)$ are called fundamental density functions of body forces, which express the stress field due to an elliptical crack in an infinite body under uniform tension σ_Z, τ_{yz}, τ_{zx}, and leads to solutions with high accuracy. In this calculation, we put $\sigma_Z^{\infty} = \tau_{yz}^{\infty}, \tau_{zx}^{\infty} = 1$. Using the expression (2), equation (1) is expressed as equation (3), whose unknowns are $F_{zz}(\xi_a,\eta_b)$, $F_{yz}(\xi_a,\eta_b)$, $F_{zx}(\xi_a,\eta_b)$, which are called weight functions. The unknown functions are related to

$$\left.\begin{aligned}
&\frac{b}{2\pi E(k)}\left[\iint\!\!\!\!\!\!=_S \frac{F_{zz}(\xi_a,\eta_b)}{r_1^3}\sqrt{1-\xi_a^2-\eta_b^2}\,\mathrm{d}\xi\,\mathrm{d}\eta\right.\\
&\qquad\left.+\iint\!\!\!\!\!\!=_S K_{zz}^{f_{zz}}(\xi,\eta,x,y,\psi)F_{zz}(\xi_a,\eta_b)\sqrt{1-\xi_a^2-\eta_b^2}\,\mathrm{d}\xi\,\mathrm{d}\eta\right]\\
&\quad+\frac{bk^2}{4\pi}\left[\frac{1}{C(k)}\iint_S K_{zz}^{f_{yz}}(\xi,\eta,x,y,\psi)F_{yz}(\xi_a,\eta_b)\sqrt{1-\xi_a^2-\eta_b^2}\,\mathrm{d}\xi\,\mathrm{d}\eta\right.\\
&\qquad\left.+\frac{1}{B(k)}\iint_S K_{zz}^{f_{zx}}(\xi,\eta,x,y,\psi)F_{zx}(\xi_a,\eta_b)\sqrt{1-\xi_a^2-\eta_b^2}\,\mathrm{d}\xi\,\mathrm{d}\eta\right]\\
&= -\cos^2\psi
\end{aligned}\right\} \tag{3a}$$

$$\left.\begin{aligned}
&\frac{b}{4\pi}\left[\frac{k^2}{C(k)}\iint_S \frac{6\nu(x-\xi)(y-\eta)}{r_1^5} F_{yz}(\xi_a,\eta_b)\sqrt{1-\xi_a^2-\eta_b^2}\,\mathrm{d}\xi\,\mathrm{d}\eta\right.\\
&\quad+\frac{k^2}{B(k)}\iint_S\left\{\frac{2(1-2\nu)}{r_1^3}+\frac{6\nu(y-\eta)^2}{r_1^5}\right\}F_{zx}(\xi_a,\eta_b)\sqrt{1-\xi_a^2-\eta_b^2}\,\mathrm{d}\xi\,\mathrm{d}\eta\Big]\\
&\quad+\frac{2(1-\nu)}{(1-2\nu)E(k)}\iint_S K_{yz}^{f_{zz}}(\xi,\eta,x,y,\psi)F_{zz}(\xi_a,\eta_b)\sqrt{1-\xi_a^2-\eta_b^2}\,\mathrm{d}\xi\,\mathrm{d}\eta\\
&\quad+\frac{k^2}{C(k)}\iint_S K_{yz}^{f_{yz}}(\xi,\eta,x,y,\psi)F_{yz}(\xi_a,\eta_b)\sqrt{1-\xi_a^2-\eta_b^2}\,\mathrm{d}\xi\,\mathrm{d}\eta\\
&\quad+\frac{k^2}{B(k)}\iint_S K_{yz}^{f_{zx}}(\xi,\eta,x,y,\psi)F_{zx}(\xi_a,\eta_b)\sqrt{1-\xi_a^2-\eta_b^2}\,\mathrm{d}\xi\,\mathrm{d}\eta\Big]\\
&=-\sin\psi\cos\psi
\end{aligned}\right\}\tag{3b}$$

$$\left.\begin{aligned}
&\frac{b}{4\pi}\left[\frac{k^2}{C(k)}\iint_S\left\{\frac{2(1-2\nu)}{r_1^3}+\frac{6\nu(x-\xi)^2}{r_1^5}\right\}F_{yz}(\xi_a,\eta_b)\sqrt{1-\xi_a^2-\eta_b^2}\,\mathrm{d}\xi\,\mathrm{d}\eta\right]\\
&\quad+\frac{k^2}{B(k)}\iint_S\frac{6\nu(x-\xi)(y-\eta)}{r_1^5}F_{zx}(\xi_a,\eta_b)\sqrt{1-\xi_a^2-\eta_b^2}\,\mathrm{d}\xi\,\mathrm{d}\eta\\
&\quad+\frac{2(1-\nu)}{(1-2\nu)E(k)}\iint_S K_{zx}^{f_{zz}}(\xi,\eta,x,y,\psi)F_{zz}(\xi_a,\eta_b)\sqrt{1-\xi_a^2-\eta_b^2}\,\mathrm{d}\xi\,\mathrm{d}\eta\\
&\quad+\frac{k^2}{C(k)}\iint_S K_{zx}^{f_{yz}}(\xi,\eta,x,y,\psi)F_{yz}(\xi_a,\eta_b)\sqrt{1-\xi_a^2-\eta_b^2}\,\mathrm{d}\xi\,\mathrm{d}\eta\\
&\quad+\frac{k^2}{B(k)}\iint_S K_{yz}^{f_{zx}}(\xi,\eta,x,y,\psi)F_{zx}(\xi_a,\eta_b)\sqrt{1-\xi_a^2-\eta_b^2}\,\mathrm{d}\xi\,\mathrm{d}\eta\Big]=0
\end{aligned}\right\}\tag{3c}$$

Since the problem is symmetric with respect to y-axis, the expressions (4) can be applied to approximate symmetric unknown functions $F_{zz}(\xi_a,\eta_b)$, $F_{yz}(\xi_a,\eta_b)$, $F_{zx}(\xi_a,\eta_b)$.

$$\begin{aligned}
F_{zz}(\xi_a,\eta_b) &= \alpha_0+\alpha_1\eta_b+\cdots+\alpha_{n-1}\eta_b^{n-1}+\alpha_n\eta_b^n\\
&\quad+\alpha_{n+1}\xi_a^{2\times1}+\alpha_{n+2}\xi_a^{2\times1}\eta_b+\cdots+\alpha_{2n}\xi_a^{2\times1}\eta_b^{n-1}\\
&\quad\vdots\qquad\qquad\vdots\\
&\quad+\alpha_{l-2}\xi_a^{2\cdot(n-1)}+\alpha_{l-1}\xi_a^{2\cdot(n-1)}\eta_b+\alpha_l\xi_a^{2\cdot n}\\
&= \sum_{i=0}^{l}\alpha_i G_i(\xi_a,\eta_b)\\
F_{yz}(\xi_a,\eta_b) &= \beta_0+\beta_1\eta_b+\cdots+\beta_{n-1}\eta_b^{n-1}+\beta_n\eta_b^n\\
&\quad+\beta_{n+1}\xi_a^{2\times1}+\beta_{n+2}\xi_a^{2\times1}\eta_b+\cdots+\beta_{2n}\xi_a^{2\times1}\eta_b^{n-1}\\
&\quad\vdots\qquad\qquad\vdots\\
&\quad+\beta_{l-2}\xi_a^{2\cdot(n-1)}+\beta_{l-1}\xi_a^{2\cdot(n-1)}\eta_b+\beta_l\xi_a^{2\cdot n}\\
&= \sum_{i=0}^{l}\beta_i G_i(\xi_a,\eta_b)
\end{aligned}\tag{4}$$

$$
\begin{aligned}
F_{zx}(\xi_a, \eta_b) \;=\; & \gamma_0\xi_a + \gamma_1\xi_a\eta_b + \cdots + \gamma_{n-1}\xi_a\eta_b^{n-1} + \gamma_n\xi_a\eta_b^{n} \\
& + \gamma_{n+1}\xi_a^{2\times1+1} + \gamma_{n+2}\xi_a^{2\times1+1}\eta_b + \cdots + \gamma_{2n}\xi_a^{2\times1+1}\eta_b^{n-1} \\
& \quad\vdots \qquad\qquad\qquad \vdots \\
& + \gamma_{l-2}\xi_a^{2\cdot(n-1)+1} + \gamma_{l-1}\xi_a^{2\cdot(n-1)+1}\eta_b + \gamma_l\xi_a^{2\cdot n+1} \\
= \; & \sum_{i=0}^{l} \gamma_i Q_i(\xi_a, \eta_b) \qquad l = \sum_{k=0}^{n}(k+1) = \frac{(n+1)(n+2)}{2}
\end{aligned}
$$

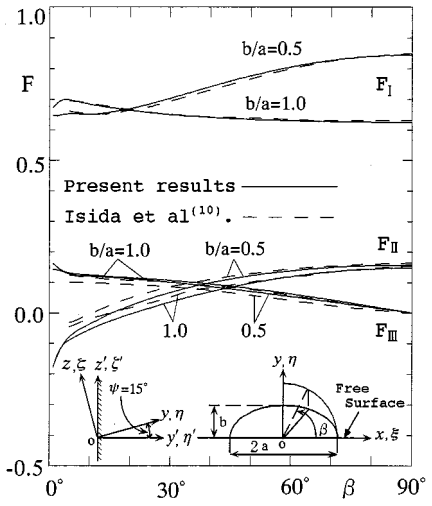

Figure 4. Variation of F_{I}, F_{II}, F_{III} along crack front in Figure 1 when $\Psi = 15$ degree, $\nu = 0.3$, $n = 20$.

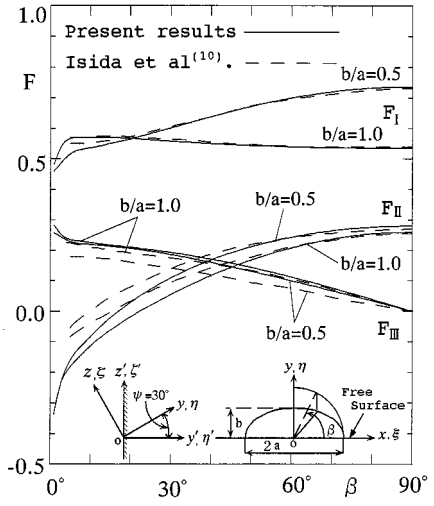

Figure 5. Variation of F_{I}, F_{II}, F_{III} along crack front in Figure 1 when $\Psi = 30$ degree, $\nu = 0.3$, $n = 20$.

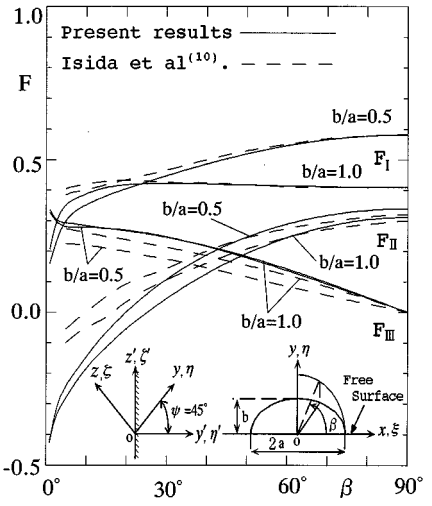

Figure 6. Variation of F_{I}, F_{II}, F_{III} along crack front in Figure 1 when $\Psi = 45$ degree, $\nu = 0.3$, $n = 20$.

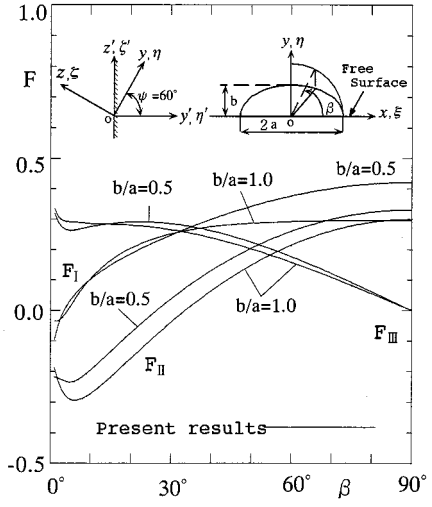

Figure 7. Variation of F_{I}, F_{II}, F_{III} along crack front in Figure 1 when $\Psi = 60$ degree, $\nu = 0.3$, $n = 20$.

$$G_0(\xi_a, \eta_b) = 1, \quad G_1(\xi_a, \eta_b) = \eta_b, \ldots, G_{n+1}(\xi_a, \eta_b) = \xi_a^{2\times 1}, \ldots,$$
$$G_l(\xi_a, \eta_b) = \xi_a^{2\cdot n}$$
$$Q_0(\xi_a, \eta_b) = \xi_a, \quad Q_1(\xi_a, \eta_b) = \xi_a \eta_b, \ldots, Q_{n+1}(\xi_a, \eta_b) = \xi_a^{2\times 1+1}, \ldots,$$
$$Q_l(\xi_a, \eta_b) = \xi_a^{2\cdot n+1}.$$

Using the approximation method mentioned above, we obtain the following system of algebraic equations for the determination of $F_{zz}(\xi_a, \eta_b)$, $F_{yz}(\xi_a, \eta_b)$, $F_{zx}(\xi_a, \eta_b)$. The unknown coefficients $\alpha_0 \sim \alpha_l, \beta_0 \sim \beta_l, \gamma_0 \sim \gamma_l [n = 1, 2, \ldots l, l = (1/2)(n+1)(n+2)]$ are then determined from (5) by selecting a set of collocation points.

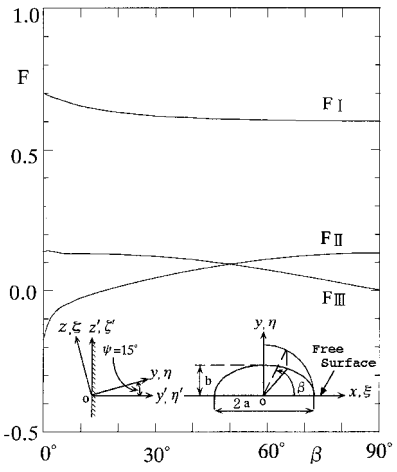

Figure 8. Variation of F_{I}, F_{II}, F_{III} along crack front in Figure 1 when $\Psi = 15$ degree, $\nu = 0.0, n = 20$.

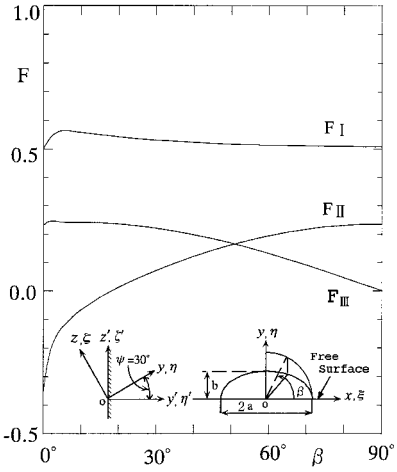

Figure 9. Variation of F_{I}, F_{II}, F_{III} along crack front in Figure 1 when $\Psi = 30$ degree, $\nu = 0.0, n = 20$.

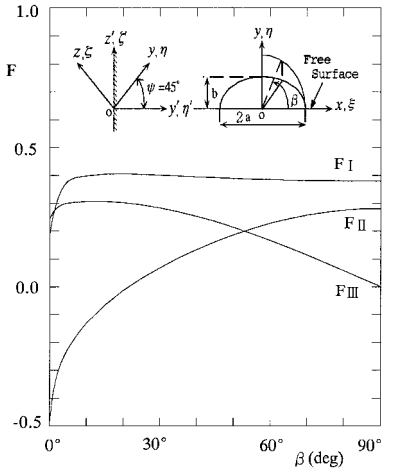

Figure 10. Variation of F_{I}, F_{II}, F_{III} along crack front in Figure 1 when $\Psi = 45$ degree, $\nu = 0.0, n = 20$.

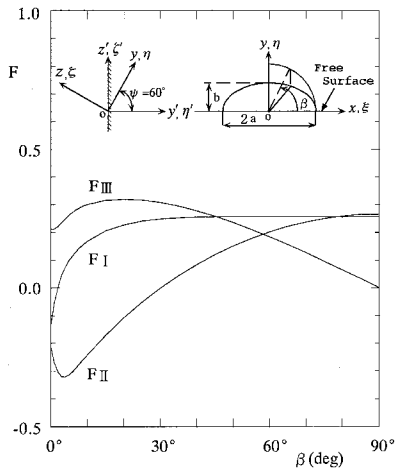

Figure 11. Variation of F_{I}, F_{II}, F_{III} along crack front in Figure 1 when $\Psi = 60$ degree, $\nu = 0.0, n = 20$.

$$\left.\begin{aligned}
&\sum_{i=0}^{l}\left[\alpha_i(A_{zz,i}^{f_{zz}}+B_{zz,i}^{f_{zz}})+\beta_i B_{zz,i}^{f_{yz}}+\gamma_i B_{zz,i}^{f_{zx}}\right]=-\cos^2\psi\\
&\sum_{i=0}^{l}\left[\alpha_i B_{yz,i}^{f_{zz}}+\beta_i(A_{yz,i}^{f_{yz}}+B_{yz,i}^{f_{yz}})+\gamma_i(A_{yz,i}^{f_{zx}}+B_{yz,i}^{f_{zx}})\right]=-\cos\psi\sin\psi\\
&\sum_{i=0}^{l}\left[\alpha_i B_{zx,i}^{f_{zz}}+\beta_i(A_{zx,i}^{f_{yz}}+B_{zx,i}^{f_{yz}})+\gamma_i(A_{zx,i}^{f_{zx}}+B_{zx,i}^{f_{zx}})\right]=0
\end{aligned}\right\}\tag{5a}$$

The number of unknowns in (5a) are $3(l+1)$. As examples, $A_{zz,i}^{f_{zz}}$, $B_{zz,i}^{f_{zz}}$, $B_{z,i}^{f_{yz}}$, $B_{zz,i}^{f_{zx}}$ are expressed as follows.

$$\left.\begin{aligned}
A_{zz,i}^{f_{zz}}&=\frac{b}{2\pi E(k)}\iint\!\!\!\!\!\!=_S\frac{G_i(\xi_a,\eta_b)}{r_1^3}\sqrt{1-\xi_a^2-\eta_b^2}\,\mathrm{d}\xi\,\mathrm{d}\eta\\
B_{zz,i}^{f_{zz}}&=\frac{b}{2\pi E(k)}\iint_S K_{zz}^{f_{zz}}(\xi,\eta,x,y,\psi)G_i(\xi_a,\eta_b)\sqrt{1-\xi_a^2-\eta_b^2}\,\mathrm{d}\xi\,\mathrm{d}\eta\\
B_{zz,i}^{f_{yz}}&=\frac{bk^2}{4\pi C(k)}\iint_S K_{zz}^{f_{yz}}(\xi,\eta,x,y,\psi)G_i(\xi_a,\eta_b)\sqrt{1-\xi_a^2-\eta_b^2}\,\mathrm{d}\xi\,\mathrm{d}\eta\\
B_{zz,i}^{f_{zx}}&=\frac{bk^2}{4\pi B(k)}\iint_S K_{zz}^{f_{zx}}(\xi,\eta,x,y,\psi)Q_i(\xi_a,\eta_b)\sqrt{1-\xi_a^2-\eta_b^2}\,\mathrm{d}\xi\,\mathrm{d}\eta
\end{aligned}\right\}\tag{5b}$$

In (5) the integral B_i can be evaluated numerically because of no singularities in the integral. However, A_i cannot be evaluated by ordinary numerical procedure because they have hypersingularites of the form r^{-3} when $x=\xi$ and $y=\eta$ (Hadamard,1923) Therefore the similar method shown in previous papers is applied (Takakuda et al., 1984, Noda–Miyashi, 1996).

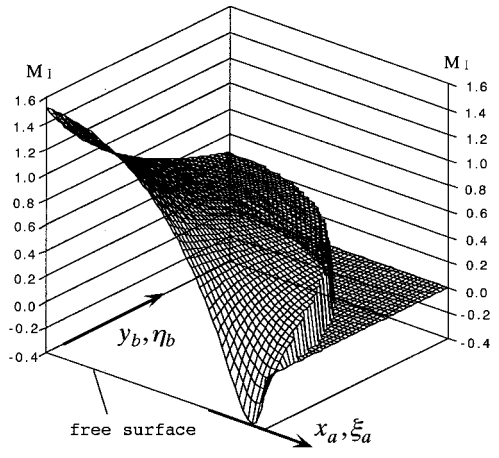

Figure 12. Crack opening displacement $M_{\mathrm{I}}(x_a, y_b)\Psi = 60$ degree, $\nu = 0.3, n = 20, b/a = 1.0$.

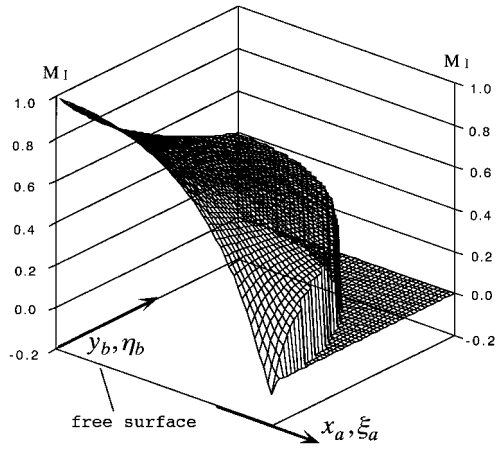

Figure 13. Crack opening displacement $M_{\mathrm{I}}(x_a, y_b)\Psi = 60$ degree, $\nu = 0.0, n = 20, b/a = 1.0$.

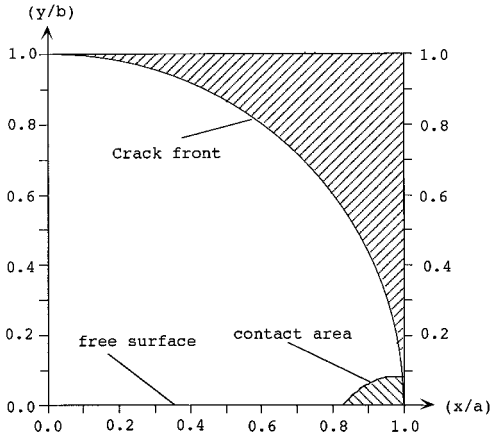

Figure 14. Contact zone of crack surface $\Psi = 60$ degree, $\nu = 0.3, n = 20, b/a = 1.0$.

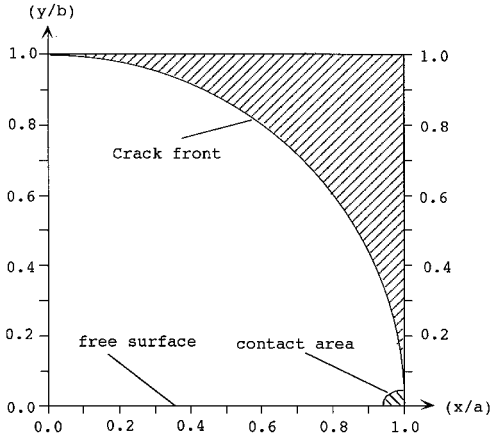

Figure 15. Contact zone of crack surface $\Psi = 60$ degree, $\nu = 0.0, n = 20, b/a = 1.0$.

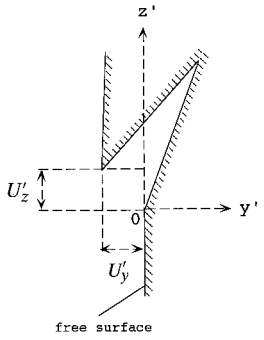

Figure 16. Definition of crack mouth opening displacement at free surface.

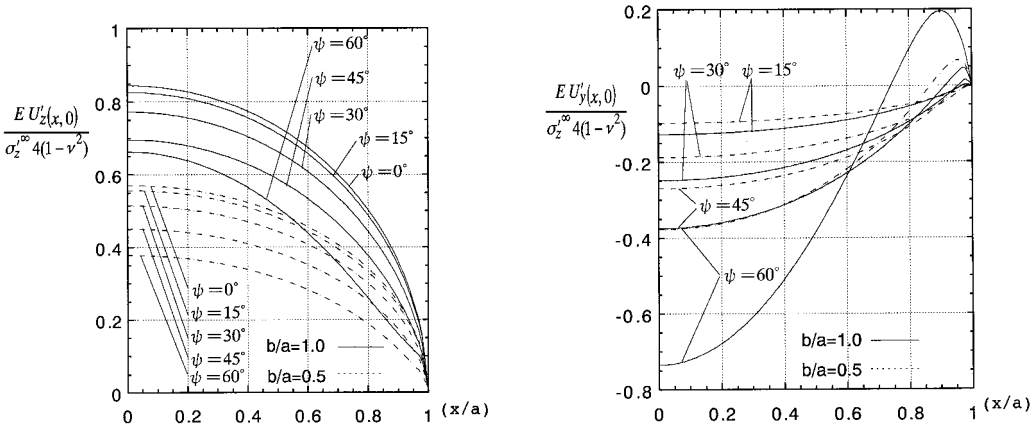

Figure 17. Crack mouth opening displacement at free surface in Figure 1 when $\nu = 0.3, n = 20$. (a) Crack mouth opening displacement in the z' direction in Figure 16. (b) Crack mouth opening displacement in the y' direction in Figure 16.

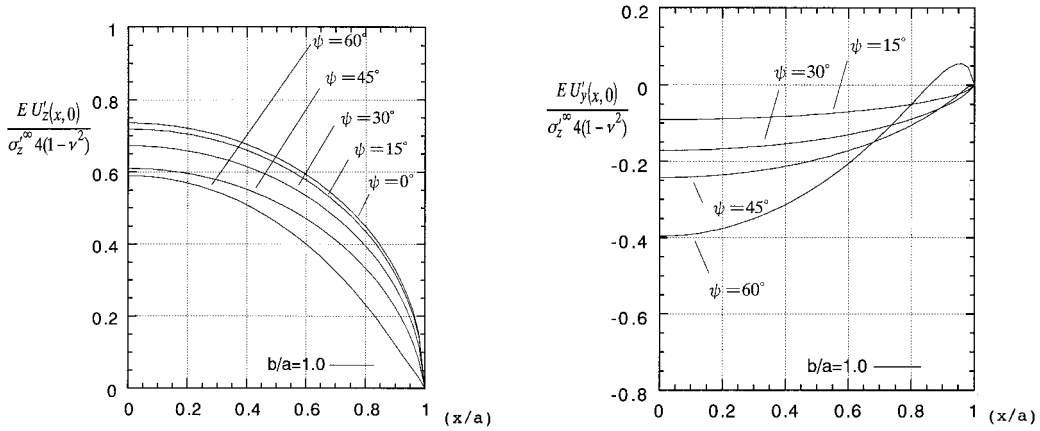

Figure 18. Crack mouth opening displacement at free surface in Figure 1 when $\nu = 0.0$, $n = 20$. (a) Crack mouth opening displacement in the z' direction in Figure 16. (b) Crack mouth opening displacement in the y' direction in Figure 16.

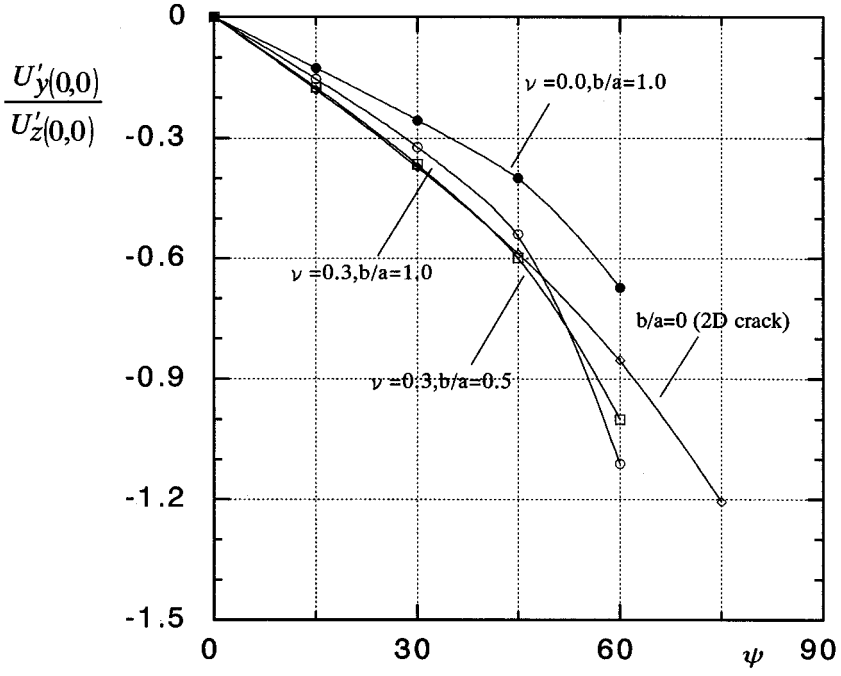

Figure 19. $Uy'(0, 0)/Uz'(0, 0)$ vs. Ψ relation.

4. Numerical results and discussion

Numerical calculations have been carried out for changing n in (4) and ψ in (1) for $b/a = 0.5$, 1.0 and $\nu = 0.0$, 0.3. Numerical integrals have been performed using scientific subroutine

library (FACOM SSL II DAQE etc.). In demonstrating the numerical results of stress intensity factors K_{I}, K_{II}, K_{III} the following dimensionless factors F_{I}, F_{II}, F_{III} will be used.

$$
\left.
\begin{aligned}
F_{\mathrm{I}}(\beta) &= \frac{K_{\mathrm{I}}(\beta)}{\sigma'^{\infty}_{z}\sqrt{\pi b}} = \frac{F_{zz}}{E(k)}\left[\sin^2\beta + \left(\frac{b}{a}\right)^2\cos^2\beta\right]^{1/4} \\
F_{\mathrm{II}}(\beta) &= \frac{K_{\mathrm{II}}(\beta)}{\sigma'^{\infty}_{z}\sqrt{\pi b}} = \left(F_{zx}\frac{k'\cos\beta}{B(k)} + F_{yz}\frac{\sin\beta}{C(k)}\right)\frac{k^2}{(1-k^2\cos^2\beta)^{1/4}} \\
F_{\mathrm{III}}(\beta) &= \frac{K_{\mathrm{III}}(\beta)}{\sigma'^{\infty}_{z}\sqrt{\pi b}} = \left(-F_{zx}\frac{\sin\beta}{B(k)} + F_{yz}\frac{k'\cos\beta}{C(k)}\right)\frac{(1-\nu)k^2}{(1-k^2\cos^2\beta)^{1/4}} \\
M_{\mathrm{I}}(x_a, y_b) &= \frac{U_z(x_a, y_b)}{U_{z'E}(x_a, y_b)} = F_{zz}(x_a, y_b) \\
M_{\mathrm{II}}(x_a, y_b) &= \frac{U_y(x_a, y_b)}{U_{y'E}(x_a, y_b)} = F_{yz}(x_a, y_b) \\
M_{\mathrm{III}}(x_a, y_b) &= \frac{U_x(x_a, y_b)}{U_{x'E}(x_a, y_b)} = F_{zx}(x_a, y_b) \\
U_{z'E}(x_a, y_b) &= \frac{4(1-\nu^2)}{E}\frac{b\sigma'^{\infty}_{z}}{E(K)}\sqrt{1-x_a^2-y_b^2} \\
U_{y'E}(x_a, y_b) &= \frac{4(1-\nu^2)}{E}\frac{bk^2\sigma'^{\infty}_{z}}{C(K)}\sqrt{1-x_a^2-y_b^2} \\
U_{x'E}(x_a, y_b) &= \frac{4(1-\nu^2)}{E}\frac{bk^2\sigma'^{\infty}_{z}}{C(K)}\sqrt{1-x_a^2-y_b^2} \\
F_{zz} &= F_{zz}(\xi_a, \eta_b)|_{\xi_a=\cos\beta, \eta_b=\sin\beta} \\
F_{yz} &= F_{yz}(\xi_a, \eta_b)|_{\xi_a=\cos\beta, \eta_b=\sin\beta} \\
F_{zx} &= F_{zx}(\xi_a, \eta_b)|_{\xi_a=\cos\beta, \eta_b=\sin\beta}
\end{aligned}
\right\} \tag{6}
$$

In previous studies, the stress intensity factors are obtained when $\Psi \leqslant 45$ degree. In general, as the inclination angle Ψ approaches 90 degree, accurate analysis is difficult because the effect of free surface on the stress intensity factors becomes larger. Similarly, the variations of stress intensity factors along the crack front are difficult to be obtained near the free surface. Considering those facts, the accuracy of present results is confirmed in detail especially for $\Psi > 45$ degree.

Figures 2 and 3 indicate the compliance of the boundary conditions along the prospective crack surface for $b/a = 1.0$, $\Psi = 60^\circ$ and $n = 20$. The remaining stress σ_z is less than 5×10^{-3} when $\nu = 0.3$ and less than 2×10^{-3} when $\nu = 0.0$. Similarly, the remaining stresses τ_{yz} and τ_{zx} are less than 8×10^{-3} when $\nu = 0.3$ and less than 3×10^{-3} when $\nu = 0.0$. Accuracy the numerical results for $\nu = 0.0$ is better than that for $\nu = 0.3$.

Tables 1 and 2 shows the convergence of F_{I}, F_{II}, F_{III} along the crack front when $b/a = 1.0$, $\Psi = 60$ degree with increasing the order of polynomials n in (4). Table 1 indicates the present results for $\nu = 0.3$ with accuracy to the third digit when $\beta = 0 \sim 9$ degree and with accuracy to the fourth digit when $\beta = 10 \sim 90$ degree. Table 2 indicates the results for $\nu = 0.0$ with accuracy to the third or fourth digit when $\beta = 0 \sim 9$ degree and with accuracy

.

Table 1. Convergence of dimensionless stress intensity factors F_{I}, F_{II}, F_{III} with incleasing the polynomial exponent n in (4) when $b/a = 1.0$, $\Psi = 60$ degree, $\nu = 0.3$ in Figure 1.

	β(deg)	1	2	3	4	5	6	7	8	9	10	15	20	25
	n													
F_{I}	17	−0.04288	−0.03693	−0.02526	−0.00898	0.01016	0.03045	0.05053	0.06949	0.08690	0.10267	0.16312	0.20414	0.23160
	18	−0.03655	−0.03372	−0.02316	−0.00712	0.01200	0.03218	0.05196	0.07052	0.08752	0.10295	0.16328	0.20407	0.23152
	19	−0.03863	−0.03542	−0.02425	−0.00744	0.01240	0.03308	0.05306	0.07157	0.08835	0.10353	0.16344	0.20386	0.23171
	20	−0.03533	−0.03387	−0.02329	−0.00651	0.01343	0.03413	0.05400	0.07229	0.08883	0.10380	0.16352	0.20381	0.23191
F_{II}	17	−0.19024	−0.23392	−0.26426	−0.28302	−0.29258	−0.29536	−0.29342	−0.28837	−0.28130	−0.27287	−0.21904	−0.15737	−0.09715
	18	−0.18999	−0.23395	−0.26444	−0.28317	−0.29261	−0.29526	−0.29327	−0.28825	−0.28125	−0.27291	−0.21900	−0.15753	−0.09717
	19	−0.18990	−0.23362	−0.26407	−0.28283	−0.29231	−0.29504	−0.29314	−0.28823	−0.28132	−0.27304	−0.21900	−0.15760	−0.09709
	20	−0.18860	−0.23295	−0.26368	−0.28253	−0.29206	−0.29485	−0.29305	−0.28822	−0.28140	−0.27325	−0.21903	−0.15753	−0.09690
F_{III}	17	0.33593	0.30927	0.29632	0.29111	0.28948	0.28902	0.28860	0.28784	0.28682	0.28573	0.28300	0.27971	0.27371
	18	0.33298	0.30773	0.29615	0.29174	0.29041	0.28989	0.28921	0.28815	0.28688	0.28565	0.28302	0.27969	0.27375
	19	0.33273	0.30674	0.29517	0.29107	0.29003	0.28967	0.28900	0.28789	0.28655	0.28531	0.28302	0.27972	0.27385
	20	0.33384	0.30730	0.29583	0.29184	0.29072	0.29012	0.28917	0.28783	0.28640	0.28515	0.28300	0.27974	0.27401

	β(deg)	30	35	40	45	50	55	60	65	70	75	80	85	90
	n													
F_{I}	17	0.25140	0.26493	0.27457	0.28141	0.28623	0.28959	0.29200	0.29376	0.29474	0.29550	0.29603	0.29655	0.29695
	18	0.25141	0.26493	0.27458	0.28145	0.28623	0.28960	0.29204	0.29366	0.29483	0.29563	0.29609	0.29630	0.29630
	19	0.25153	0.26494	0.27465	0.28142	0.28625	0.28957	0.29207	0.29366	0.29486	0.29564	0.29608	0.29621	0.29606
	20	0.25162	0.26492	0.27464	0.28141	0.28625	0.28958	0.29201	0.29368	0.29485	0.29562	0.29606	0.29613	0.29606
F_{II}	17	−0.03914	0.01438	0.06378	0.10841	0.14844	0.18378	0.21432	0.24030	0.26141	0.27802	0.28977	0.29672	0.29915
	18	−0.03917	0.01434	0.06371	0.10832	0.14841	0.18362	0.21433	0.24023	0.26147	0.27799	0.28974	0.29693	0.29927
	19	−0.03924	0.01434	0.06366	0.10827	0.14837	0.18359	0.21431	0.24020	0.26147	0.27793	0.28970	0.29669	0.29886
	20	−0.03926	0.01435	0.06362	0.10833	0.14834	0.18361	0.21424	0.24024	0.26144	0.27788	0.28972	0.29678	0.29920
F_{III}	17	0.26490	0.25286	0.23844	0.22132	0.20221	0.18105	0.15827	0.13407	0.10864	0.08237	0.05529	0.02773	0.00000
	18	0.26483	0.25296	0.23843	0.22144	0.20222	0.18101	0.15828	0.13404	0.10868	0.08234	0.05530	0.02770	0.00000
	19	0.26480	0.25302	0.23843	0.22148	0.20223	0.18102	0.15827	0.13402	0.10869	0.08235	0.05531	0.02771	0.00000
	20	0.26480	0.25303	0.23843	0.22148	0.20219	0.18104	0.15823	0.13406	0.10868	0.08234	0.05531	0.02771	0.00000

to the fourth or fifth digit when $\beta = 10 \sim 90$ degree. Convergence of the results when $\nu = 0.0$ is better than that when $\nu = 0.3$.

Tables 3, 4, 5 show the values of F_{I}, F_{II}, F_{III} along the crack front when $b/a = 1.0, 0.5$ and $\Psi = 15, 30, 45, 60$ degree. When $\Psi = 60$ degree, F_{I} has negative value near free surface. The actual crack surface ϕs when $\Psi = 60$ degree, therefore, seems to contact each other near the free surface.

Figures 4–7 show the values F_{I}, F_{II}, F_{III} for $\nu = 0.3$ along the crack front in comparison with Ishida et al. (1990). The result of Ishida et al. is analyzed when $\Psi \leqslant 45°$. The results

.

Table 2. Convergence of dimensionless stress intensity factors F_{I}, F_{II}, F_{III} with incleasing the polynomial exponent n in (4) when $b/a = 1.0$, $\Psi = 60$ degree, $\nu = 0.0$ in Figure 1.

	β(deg)	0	1	2	3	4	5	6	7	8	9	10	15	20	25
	n														
F_{I}	17	−0.14739	−0.06333	−0.00347	0.03956	0.07120	0.09528	0.11439	0.13022	0.14380	0.15575	0.16641	0.20532	0.22755	0.24050
	18	−0.14821	−0.06360	−0.00357	0.03944	0.07101	0.09504	0.11415	0.13001	0.14365	0.15566	0.16637	0.20535	0.22756	0.24046
	19	−0.14637	−0.06118	−0.00143	0.04107	0.07217	0.09584	0.11471	0.13040	0.14392	0.15582	0.16645	0.20539	0.22751	0.24035
	20	−0.14027	−0.05600	0.00270	0.04417	0.07432	0.09722	0.11551	0.13082	0.14409	0.15587	0.16645	0.20543	0.22749	0.24035
F_{II}	17	−0.21442	−0.27297	−0.30678	−0.32164	−0.32310	−0.31593	−0.30383	−0.28936	−0.27409	−0.25884	−0.24390	−0.17271	−0.10825	−0.05209
	18	−0.21318	−0.27350	−0.30790	−0.32268	−0.32379	−0.31627	−0.30394	−0.28939	−0.27415	−0.25895	−0.24404	−0.17249	−0.10825	−0.05205
	19	−0.20716	−0.27039	−0.30650	−0.32206	−0.32345	−0.31600	−0.30370	−0.28921	−0.27405	−0.25893	−0.24404	−0.17236	−0.10830	−0.05177
	20	−0.21023	−0.26876	−0.30375	−0.31975	−0.32198	−0.31525	−0.30340	−0.28913	−0.27403	−0.25890	−0.24400	−0.17246	−0.10842	−0.05175
F_{III}	17	0.21498	0.21670	0.22541	0.23735	0.25000	0.26190	0.27238	0.28126	0.28868	0.29486	0.30006	0.31598	0.32021	0.31723
	18	0.21688	0.21721	0.22557	0.23758	0.25037	0.26235	0.27280	0.28160	0.28891	0.29500	0.30014	0.31594	0.32019	0.31728
	19	0.21469	0.21531	0.22424	0.23687	0.25019	0.26252	0.27316	0.28202	0.28930	0.29532	0.30037	0.31593	0.32025	0.31729
	20	0.21027	0.21186	0.22172	0.23515	0.24911	0.26189	0.27281	0.28183	0.28920	0.29527	0.30035	0.31595	0.32033	0.31735

	β(deg)	30	35	40	45	50	55	60	65	70	75	80	85	90
	n													
F_{I}	17	0.24832	0.25289	0.25540	0.25671	0.25719	0.25722	0.25699	0.25657	0.25619	0.25585	0.25551	0.25524	0.25513
	18	0.24833	0.25288	0.25541	0.25673	0.25718	0.25725	0.25697	0.25657	0.25620	0.25584	0.25551	0.25514	0.25495
	19	0.24835	0.25287	0.25542	0.25671	0.25718	0.25724	0.25696	0.25657	0.25620	0.25585	0.25555	0.25538	0.25537
	20	0.24838	0.25287	0.25543	0.25671	0.25720	0.25723	0.25695	0.25659	0.25617	0.25585	0.25555	0.25543	0.25550
F_{II}	17	−0.00136	0.04341	0.08350	0.11897	0.15038	0.17776	0.20143	0.22135	0.23752	0.25016	0.25915	0.26460	0.26647
	18	−0.00135	0.04340	0.08346	0.11894	0.15036	0.17775	0.20144	0.22131	0.23754	0.25017	0.25915	0.26456	0.26633
	19	−0.00129	0.04350	0.08346	0.11899	0.15037	0.17776	0.20144	0.22131	0.23757	0.25015	0.25915	0.26444	0.26612
	20	−0.00129	0.04349	0.08347	0.11898	0.15037	0.17777	0.20142	0.22133	0.23757	0.25016	0.25914	0.26438	0.26607
F_{III}	17	0.30834	0.29505	0.27810	0.25816	0.23557	0.21080	0.18405	0.15577	0.12623	0.09546	0.06413	0.03217	0.00000
	18	0.30833	0.29508	0.27813	0.25821	0.23559	0.21079	0.18408	0.15581	0.12620	0.09548	0.06410	0.03210	0.00000
	19	0.30832	0.29504	0.27815	0.25816	0.23559	0.21080	0.18409	0.15582	0.12615	0.09555	0.06410	0.03224	0.00000
	20	0.30832	0.29505	0.27813	0.25817	0.23558	0.21081	0.18409	0.15578	0.12616	0.09557	0.06417	0.03234	0.00000

are in agreement with the present result in $30° \leqslant \beta \leqslant 45°$ except near the free surface. When $\nu = 0.0$, the values of F_{I}, F_{II}, F_{III} are shown in Figures 8–11.

Figures 12 and 13 show the crack opening displacement $M_{\mathrm{I}}(x', y')$ for $\Psi = 60$ degree and $b/a = 1.0$. It is found that $M_{\mathrm{I}}(x', y')$ has negative value in the limited region near free surface. Actual crack surface seems to contact each other near the free surface. Figures 14 and 15 indicates the contact zone for Poission's ratio $\nu = 0.0$, 0,3.

Crack mouth opening displacements defined in Figure 16 were shown in Figures 17 and 18 for $b/a = 1.0$, 0.5 and $\phi = 15$, 30, 45, 60 degrees. By measuring the displacements and using Figures 17 and 18, we can roughly estimate the crack depth. The ratio $Uy'(0, 0)/Uz'(0, 0)$

.

Table 3. Dimensionless stress intensity factors F_{I}, F_{II}, F_{III} along crack front in Figure 1 when $b/a = 1.0$, $\nu = 0.3$

	β(deg)	1	2	3	4	5	6	7	8	9	10	15	20	25
	Ψ(deg)													
F_{I}	15	0.673	0.688	0.096	0.699	0.698	0.695	0.692	0.688	0.686	0.683	0.6724	0.6635	0.6560
	30	0.479	0.517	0.542	0.557	0.565	0.569	0.570	0.570	0.570	0.570	0.5701	0.5668	0.5624
	45	0.198	0.262	0.304	0.331	0.349	0.360	0.370	0.376	0.382	0.387	0.4081	0.4174	0.4211
	60	−0.035	−0.034	−0.023	−0.007	0.013	0.034	0.054	0.072	0.089	0.103	0.1635	0.2038	0.2316
F_{II}	15	−0.179	−0.137	−0.113	−0.099	−0.089	−0.082	−0.075	−0.068	−0.061	−0.055	−0.0282	−0.0051	+0.0156
	30	−0.335	−0.266	−0.226	−0.201	−0.183	−0.168	−0.154	−0.140	−0.127	−0.114	−0.0633	−0.0193	+0.0192
	45	−0.418	−0.362	−0.327	−0.302	−0.280	−0.260	−0.239	−0.220	−0.201	−0.184	−0.1148	−0.0544	−0.0026
	60	−0.188	−0.233	−0.264	−0.282	−0.292	−0.295	−0.293	−0.288	−0.281	−0.273	−0.2190	−0.1575	−0.0970
F_{III}	15	0.162	0.149	0.140	0.133	0.130	0.128	0.127	0.126	0.124	0.124	0.1186	0.1149	0.1104
	30	0.283	0.262	0.248	0.240	0.236	0.233	0.230	0.229	0.227	0.225	0.2163	0.2093	0.2012
	45	0.335	0.311	0.299	0.296	0.293	0.291	0.289	0.287	0.285	0.283	0.2747	0.2662	0.2565
	60	0.334	0.307	0.296	0.292	0.291	0.289	0.289	0.288	0.286	0.285	0.2830	0.2797	0.2740

	β(deg)	30	35	40	45	50	55	60	65	70	75	80	85	90
	Ψ(deg)													
F_{I}	15	0.6495	0.6446	0.6404	0.6370	0.6341	0.6318	0.6298	0.6282	0.6270	0.6261	0.6255	0.6252	0.6253
	30	0.5578	0.5538	0.5500	0.5468	0.5439	0.5415	0.5394	0.5377	0.5363	0.5353	0.5354	0.5339	0.5337
	45	0.4223	0.4220	0.4208	0.4192	0.4176	0.4160	0.4144	0.4131	0.4119	0.4111	0.4105	0.4103	0.4105
	60	0.2516	0.2649	0.2746	0.2814	0.2862	0.2895	0.2920	0.2936	0.2948	0.2956	0.2960	0.2961	0.2960
F_{II}	15	0.0345	0.5217	0.0684	0.0831	0.0964	0.1082	0.1185	0.1273	0.1345	0.1401	0.1441	0.1465	0.1472
	30	0.0543	0.0867	0.1163	0.1431	0.1673	0.1887	0.2074	0.2232	0.2362	0.2464	0.2537	0.2579	0.2593
	45	0.0446	0.0873	0.1262	0.1611	0.1925	0.2201	0.2442	0.2646	0.2813	0.2943	0.3037	0.3092	0.3111
	60	−0.0392	0.0143	0.0636	0.1083	0.1483	0.1836	0.2143	0.2402	0.2614	0.2779	0.2897	0.2967	0.2991
F_{III}	15	0.1059	0.1004	0.0941	0.0872	0.0794	0.0709	0.0619	0.0524	0.0425	0.0321	0.0216	0.0107	0.0000
	30	0.1924	0.1823	0.1707	0.1579	0.1436	0.1282	0.1119	0.0964	0.0767	0.0580	0.0390	0.0194	0.0000
	45	0.2449	0.2319	0.2168	0.2004	0.1821	0.1625	0.1417	0.1198	0.0969	0.0739	0.0493	0.0247	0.0000
	60	0.2648	0.2530	0.2384	0.2215	0.2022	0.1810	0.1582	0.1341	0.1087	0.0823	0.0553	0.0277	0.0000

vs. ϕ relations are shown in Figure 19. We can easily estimate the inclination angle ϕ by measuring $Uy'(0,0)/Uz'(0,0)$ and using Figure 19.

5. Conclusion

In this paper, a singular integral equation method is applied to calculate the variation of the stress intensity factor along the crack front of a 3D inclined semi-elliptical surface crack. The conclusions can be made as follows.

.

Table 4. Dimensionless stress intensity factors F_{I}, F_{II}, F_{III} along crack front in Figure 1 when $b/a = 0.5$, $\nu = 0.3$

	β(deg)	1	2	3	4	5	6	7	8	9	10	15	20	25
	Ψ(deg)													
F_{I}	15	0.647	0.646	0.647	0.651	0.653	0.653	0.653	0.652	0.651	0.651	0.6567	0.6685	0.6845
	30	0.0460	0.475	0.491	0.505	0.516	0.523	0.528	0.531	0.533	0.536	0.5495	0.5651	0.5824
	45	0.162	0.209	0.247	0.277	0.300	0.316	0.328	0.338	0.345	0.352	0.3810	0.4047	0.4264
	60	−0.093	−0.046	−0.011	+0.014	0.034	0.051	0.065	0.079	0.091	0.102	0.1486	0.1861	0.2182
F_{II}	15	−0.177	−0.142	−0.115	−0.094	−0.079	−0.068	−0.059	−0.051	−0.045	−0.038	−0.0437	+0.0226	+0.0460
	30	−0.335	−0.271	−0.223	−0.118	−0.162	−0.142	−0.126	−0.111	−0.098	−0.084	−0.0226	+0.0279	+0.0714
	45	−0.425	−0.351	−0.301	−0.268	−0.242	−0.221	−0.202	−0.183	−0.165	−0.417	−0.0664	−0.0007	+0.0582
	60	−0.218	−0.221	−0.228	−0.234	−0.235	−0.233	−0.227	−0.218	−0.207	−0.196	−0.1357	−0.0742	−0.0163
F_{III}	15	0.142	0.140	0.136	0.131	0.127	0.124	0.122	0.121	0.120	0.120	0.1160	0.1114	0.1062
	30	0.257	0.249	0.241	0.234	0.228	0.244	0.222	0.220	0.220	0.219	0.2132	0.2057	0.1967
	45	0.326	0.306	0.292	0.284	0.280	0.278	0.277	0.278	0.278	0.278	0.2745	0.2684	0.2589
	60	0.318	0.289	0.272	0.264	0.263	0.264	0.266	0.269	0.272	0.275	0.2847	0.2901	0.2898

	β(deg)	30	35	40	45	50	55	60	65	70	75	80	85	90
	Ψ(deg)													
F_{I}	15	0.7024	0.7214	0.7403	0.7585	0.7755	0.7911	0.8049	0.8168	0.8267	0.8344	0.8400	0.8433	0.8444
	30	0.6007	0.6194	0.6375	0.6549	0.6711	0.6858	0.6987	0.7099	0.7191	0.7264	0.7317	0.7348	0.7357
	45	0.4470	0.4668	0.4854	0.5028	0.5188	0.5332	0.5458	0.5567	0.5656	0.5725	0.5776	0.5805	0.5816
	60	0.2473	0.2739	0.2986	0.3211	0.3416	0.3599	0.3758	0.3894	0.4006	0.4093	0.4156	0.4192	0.4204
F_{II}	15	0.659	0.0830	0.0977	0.1103	0.1210	0.1302	0.1377	0.1440	0.1491	0.1529	0.1555	0.1571	0.1577
	30	+0.1085	0.1404	0.1678	0.1913	0.2112	0.2282	0.2424	0.2541	0.2635	0.2707	0.2756	0.2786	0.2797
	45	+0.1077	0.1503	0.1871	0.2188	0.2460	0.2691	0.2885	0.3046	0.3175	0.3273	0.3343	0.3384	0.3399
	60	+0.0374	0.0861	0.1301	0.1694	0.2039	0.2340	0.2599	0.2816	0.2992	0.3128	0.3225	0.3284	0.3303
F_{III}	15	0.1000	0.0932	0.0858	0.0780	0.0700	0.0617	0.0531	0.0445	0.0357	0.0269	0.0180	0.0092	0.0000
	30	0.1857	0.1735	0.1601	0.1459	0.1310	0.1156	0.0997	0.0836	0.0672	0.0505	0.0338	0.0170	0.0000
	45	0.2465	0.2318	0.2152	0.1972	0.1778	0.1575	0.1364	0.1146	0.0923	0.0695	0.0464	0.0233	0.0000
	60	0.2847	0.2750	0.2614	0.2443	0.2242	0.2015	0.1766	0.1499	0.1217	0.0921	0.0619	0.0310	0.0000

(1) The analysis of mixed mode 3D cracks is more difficult than the analysis of mode I 3D cracks because of triple number of unknown functions and boundary conditions. In particular, to obtain accurate stress intensity factors near the free surface for large inclination angles ($\psi > 45$ degrees) is difficult because the effect of free surface on the results is complicated.

(2) In the numerical calculation, the unknown body force densities are approximated by using fundamental density functions and polynomials. Then, the calculations show that the present method yields good convergence of the results and highly satisfied boundary conditions. Smooth variations of stress intensity factors along the crack front were indicated

.

Table 5. Dimensionless stress intensity factors F_{I}, F_{II}, F_{III} along crack front in Figure 1 when $b/a = 1.0$, $\nu = 0.0$ in

	β(deg)	0	1	2	3	4	5	6	7	8	9	10	15	20	25
	υ(deg)														
F_{I}	15	0.7007	0.6932	0.6879	0.6835	0.6791	0.6747	0.6703	0.6659	0.6618	0.6580	0.6545	0.6411	0.6316	0.6246
	30	0.5007	0.5231	0.5406	0.5525	0.5595	0.5625	0.5629	0.5617	0.5599	0.5579	0.5560	0.5485	0.5415	0.5354
	45	0.1851	0.2559	0.3074	0.3426	0.3652	0.3789	0.3868	0.3913	0.3941	0.3962	0.3980	0.4046	0.4052	0.4033
	60	−0.1403	−0.0560	0.0027	0.0442	0.0743	0.0972	0.1155	0.1308	0.1441	0.1559	0.1665	0.2054	0.2275	0.2404
F_{II}	15	−0.1731	−0.1253	−0.0959	−0.0777	−0.0658	−0.0571	−0.0499	−0.0435	−0.0374	−0.0317	−0.0264	−0.0046	+0.0138	+0.0300
	30	−0.3556	−0.2625	−0.2055	−0.1702	−0.1467	−0.1292	−0.1145	−0.1011	−0.0887	−0.0770	−0.0663	−0.0228	+0.0133	+0.0443
	45	−0.4870	−0.3811	−0.3171	−0.2764	−0.2474	−0.2238	−0.2026	−0.1828	−0.1642	−0.1471	−0.1313	−0.0674	−0.0152	+0.0283
	60	−0.2102	−0.2688	−0.3038	−0.3198	−0.3220	−0.3153	−0.3034	−0.2891	−0.2740	−0.2589	−0.2440	−0.1725	−0.1084	−0.0518
F_{III}	15	0.1385	0.1417	0.1404	0.1375	0.1347	0.1327	0.1316	0.1311	0.1311	0.1312	0.1314	0.1305	0.1284	0.1252
	30	0.2299	0.2424	0.2460	0.2454	0.2435	0.2417	0.2407	0.2403	0.2403	0.2406	0.2408	0.2393	0.2352	0.2289
	45	0.2436	0.2688	0.2837	0.2923	0.2972	0.3000	0.3018	0.3032	0.3045	0.3056	0.3065	0.3069	0.3021	0.2939
	60	0.2103	0.2119	0.2217	0.2352	0.2491	0.2619	0.2728	0.2818	0.2892	0.2953	0.3004	0.3160	0.3203	0.3174

	β(deg)	30	35	40	45	50	55	60	65	70	75	80	85	90
	υ(deg)													
F_{I}	15	0.6191	0.6150	0.6117	0.6091	0.6071	0.6054	0.6041	0.6031	0.6023	0.6018	0.6013	0.6011	0.6010
	30	0.5299	0.5255	0.5217	0.5185	0.5159	0.5138	0.5119	0.5105	0.5093	0.5085	0.5079	0.5075	0.5074
	45	0.4004	0.3973	0.3942	0.3914	0.3889	0.3867	0.3847	0.3831	0.3817	0.3808	0.3801	0.3796	0.3796
	60	0.2484	0.2529	0.2554	0.2567	0.2572	0.2572	0.2570	0.2566	0.2562	0.2559	0.2556	0.2554	0.2555
F_{II}	15	0.0449	0.0586	0.0712	0.0827	0.0931	0.1025	0.1107	0.1176	0.1234	0.1280	0.1312	0.1334	0.1341
	30	0.0723	0.0978	0.1212	0.1423	0.1614	0.1784	0.1933	0.2059	0.2164	0.2246	0.2305	0.2343	0.2357
	45	0.0672	0.1017	0.1329	0.1608	0.1859	0.2080	0.2272	0.2435	0.2569	0.2673	0.2748	0.2796	0.2813
	60	−0.0013	0.0435	0.0835	0.1190	0.1504	0.1778	0.2014	0.2213	0.2376	0.2502	0.2591	0.2644	0.2661
F_{III}	15	0.1211	0.1157	0.1091	0.1014	0.0927	0.0832	0.0728	0.0618	0.0501	0.0380	0.0255	0.0128	0.0000
	30	0.2206	0.2103	0.1978	0.1837	0.1677	0.1502	0.1314	0.1114	0.0903	0.0684	0.0459	0.0231	0.0000
	45	0.2824	0.2686	0.2521	0.2335	0.2127	0.1903	0.1661	0.1406	0.1139	0.0863	0.0579	0.0292	0.0000
	60	0.3083	0.2951	0.2781	0.2582	0.2356	0.2108	0.1841	0.1558	0.1262	0.0956	0.0642	0.0323	0.0000

in Tables 1–5 and Figures 2–11 with varying the inclination angle, elliptical shape, and Poisson's ratio.

(3) Crack mouth opening displacements were shown in Figures 17, 18, and 19 for several inclination angles and crack depths. By measuring the displacements and using these figures it is possible to predict the crack depth and inclination angle.

(4) When the inclination angle $\Psi = 60$ degree, the mode I stress intensity factor F_{I} has negative value in the limited region near free surface. The crack surface seems to contact each other near the surface.

References

Hadamard, J. (1923). *Lectures on Caunchy's Problem in Linear Partical Differential Equations*, Yale Univ. Press.

Isida, M. and Noguchi, H. (1982a). Tension and bending of a plate with a semi-elliptical surface crack. *Transactions of the Japan Society of Mechanical Engineers* **48**A, 607–619 (in Japanese).

Isida, M. and Noguchi, H. (1982b). Analysis of three-dimensional crack problems using body force method. *Transactions of the Japan Society of Mechanical Engineers* **49**A, 707–717 (in Japanese).

Isida, M., Tokumoto, A. and Noguchi, H. (1982). Oblique semi-elliptical surface crack in semi-infinite solid subjected to tension. *Proceedings of Japan Society of Mechanical Engineers*, No. 838-1, 4–6 (in Japanese).

Isida, M., Tokumoto, A. and Noguchi, H. (1990). Oblique semi-elliptical surface crack in semi-infinite solid subjected to tension. *Engineering of Fracture Mechanics* **36-6**, 889–892.

Isida, M., Tsuru, H. and Noguchi, H. (1993a). New method of analysis of three-dimensional crack problems (1st Report, Basic theory and applications to infinite body problems). *Transactions of the Japan Society of Mechanical Engineers* **59**A, 1270–1278 (in Japanese).

Isida, M., Tsuru, H. and Noguchi, H. (1993b). New method of analysis of three-dimensional crack problems (2nd Report, Application to semi-Infinite body problems with an arbitrary surface or internal crack under complex loading conditions). *Transactions of the Japan Society of Mechanical Engineers* **59**A, 1279–1286 (in Japanese).

Murakami, Y. (1985). Analysis of stress intensity factors of modes I, II and III inclined surface cracks of arbitrary shape. *Engineering of Fracture Mechanics* **22-1**, 101–114.

Murakami, Y. and Sakae, C. (1992). Analysis of stress intensity factors for a three-dimensional bent surface crack. *Journal of The Society of Materials* **41**, No. 467, 1214–1220 (in Japanese).

Murakami, Y. and Isida, M. (1984). Analysis of mixed mode stress intensity factor $K_{\mathrm{I}}, K_{\mathrm{II}}, K_{\mathrm{III}}$ of oblique arbitrary surface crack. *Transactions of the Japan Society of Mechanical Engineers* **50**A, 1359–1366 (in Japanese).

Nisitani, H. (1967). The two-dimensional stress problem solved using an electric digital computer. *Journal of Japan Society of Mechanical Engineers*, **70**, 627–632 (in Japanese).

Nisitani, H. (1968). *Bulletin of Japan Society of Mechanical Engineers* **11**, 14–23.

Nisitani, H. and Murakami, Y. (1974a). Stress intensity factor of elliptical and semi-elliptical cracks in plates subjected to tension. *Transactions of the Japan Society of Mechanical Engineers* **40**, 31–40. (in Japanese).

Nisitani, H. and Murakami, Y. (1974b). Stress intensity factor of an elliptical crack and semi-elliptical crack in plates subjected to tension. *International Journal of Fracture* **10**, 353–368.

Noda, N.-A. and Oda, K. (1992). Numerical solution of the singular integral equations in the crack analysis using the body force method. *International Journal of Fracture* **58**, 285–304.

Noda, N.-A. and Miyoshi, S. (1996). Variation of stress intensity factor and crack opening displacement of semi-elliptical surface crack. *International Journal of Fracture* **75**, 19–48.

Takakuda, H., Koizumi, T. and Shibuya, T. (1984). On the solution of integral equations for crack problems. *Transactions of the Japan Society of Mechanical Engineers* **50**A, 1184–1192 (in Japanese).